Biosensors and Bioelectronics 131 (2019) 267–273

Contents lists available at ScienceDirect

Biosensors and Bioelectronics

journal homepage: www.elsevier.com/locate/bios

Ultrasensitive electrochemical detection of microRNA-21 with wide linear dynamic range based on dual signal amplification

Wen-Jing Guo[a], Zhen Wu[b], Xiao-Yan Yang[a], Dai-Wen Pang[a], Zhi-Ling Zhang[a,*]

[a] Key Laboratory of Analytical Chemistry for Biology and Medicine (Ministry of Education), College of Chemistry and Molecular Sciences, Wuhan University, Wuhan 430072, PR China

[b] Hubei Collaborative Innovation Center for Advanced Organic Chemical Materials, Ministry of Education Key Laboratory for the Synthesis and Application of Organic Functional Molecules, College of Chemistry and Chemical Engineering, Hubei University, Wuhan 430062, PR China

ARTICLE INFO

Keywords:
MicroRNA-21
Hybridization chain reaction
Enzyme-induced metallization
Anodic stripping voltammetry
Microelectrode array

ABSTRACT

Abnormal expression of microRNAs is closely related to human diseases. Ultrasensitive detection of microRNAs with wide linear dynamic range is necessary as the concentrations of microRNAs distributed in biological samples usually range from fM to nM. Here, we constructed an ultrasensitive electrochemical sensor for microRNA-21 based on the integration of a dual signal amplification strategy of hybridization chain reaction (HCR) and enzyme-induced metallization (EIM) with anodic stripping voltammetry (ASV). MicroRNA-21 was captured by capture probe H1 (CP H1) modified magnetic nanobeads (MBs) and amplified by HCR. Multiple alkaline phosphatases (ALP) were coupled based on the specific reaction of biotin and streptavidin. A dual amplification strategy of HCR and EIM enhanced electrochemical signal by approximately 120-fold from the perspectives of target amplification and detection signal amplification, which decreased the detection limit of microRNA-21 to 0.12 fM. Compared to the reports previously reported, a wider linear dynamic range of 2.5 fM to 25 nM spanning 7 orders of magnitude was obtained. The method provides high sensitivity, specificity and a wider linear dynamic range, which shows a great potential in the early diagnosis of diseases.

1. Introduction

MicroRNAs are a kind of noncoding small RNA molecules with a length of 18–24 nucleotides, which were firstly reported in C. elegans by Wightman in 1993 (Wightman et al., 1993). MicroRNAs participate in the regulation of individual development, cell apoptosis, proliferation and differentiation (Johnston, Hobert, 2003; Lu et al., 2005; Brennecke et al., 2003; Wienholds et al., 2005). There are many unique characteristics of microRNAs such as small size, high homology, low abundance, difficult extraction, which pose analytical challenges for their accurate detection and quantification. Therefore, the detection method must have high sensitivity and specificity. Traditional detection methods for microRNAs include northern blot (Varallyay et al., 2008), microarray chip (Thomson et al., 2004), quantitative reverse transcription-polymerase chain reaction (qRT-PCR) (Rui, Chiang, 2005) and new generation sequencing (NGS) (Shirley et al., 2014). However, low sensitivity, complex operation, poor specificity or expensive instruments limit the wide application of these methods. Therefore, it is necessary to build a sensitive biosensor for the detection of microRNAs. A growing number of studies showed that MicroRNA-21 is widely distributed in cells and tissues of breast cancer (Frankel et al., 2008), gastric cancer (Zhang et al., 2008), glioma (Galina et al., 2008), cervical cancer (Yao et al., 2009), prostate cancer (Folini et al., 2010) and lung cancer (Zhang et al., 2010). Yang et al. (2018) found that the concentrations of microRNAs widely distributed in biological samples usually range from fM to nM across 6 orders of magnitude, which require a wide linear dynamic range of detection methods. Therefore, it is necessary to develop a detection method for microRNAs, which not only has a high sensitivity, but also has a wider linear dynamic range.

In clinical diagnosis, the concentrations of target nucleic acids are too low to obtain the detection signal. On one hand, a series of strategies from the perspective of target amplification are introduced to achieve sensitive detection of nucleic acids, such as polymerase chain reaction (PCR) (Jung et al., 2018), rolling circle amplification (RCA) (Xu et al., 2018), loop-mediated isothermal amplification (LAMP) (Salamin et al., 2017), catalytic hairpin assembly (CHA) (Tang et al., 2018) and hybridization chain reaction (HCR) (Mansourian et al., 2017) and so on. Among them, HCR is an isothermal, enzyme-free nucleic acids amplification technique proposed by Dirks and Pierce (2004). In a typical HCR, the initiator triggers a cascade hybridization

* Corresponding author.
E-mail address: zlzhang@whu.edu.cn (Z.-L. Zhang).

https://doi.org/10.1016/j.bios.2019.02.026
Received 3 December 2018; Received in revised form 18 January 2019; Accepted 11 February 2019
Available online 19 February 2019
0956-5663/

chain reaction of two hairpin nucleic acids molecules to form alternate nucleic acids polymers. Due to mild reaction conditions, simple operation, high amplification efficiency, HCR has been widely used in the electrochemical, fluorescence and colorimetric detection of nucleic acids (Yuan et al., 2017; Torrente-Rodríguez et al., 2016; Ge et al., 2014; Hou et al., 2015; Yang et al., 2012; Yu et al., 2015) as an effective nucleic acids amplification technique.

On the other hand, some signal amplification strategies from the perspective of detection signal amplification based on nanomaterial and enzyme are also widely used in the detection of nucleic acids. Due to excellent catalytic activity, nanozyme (Gao et al., 2007; Park et al., 2002) and enzyme (Alfonta et al., 2001; Rochelet-Dequaire et al., 2009) are often used as signal markers to improve detection sensitivity. Robert et al. (2005) found that enzyme-induced metallization (EIM) not only has the high amplification effect of nanoparticle labels in combination with metal enhancement, but also has the specificity of enzymatic catalytic reaction, which greatly reduces the background signal and significantly improves the detection sensitivity. EIM has been used to achieve electrochemical and colorimetric detection of the viruses (Zhou et al., 2015, 2014) and nucleic acids (Hwang et al., 2005). Wu et al. decreased the detection limit of alkaline phosphatases (ALP) to 1 aM based on the combination of EIM and anodic stripping voltammetry (ASV), which proposed an effective signal amplification method (Wu et al., 2016). In view of the above, a more effective dual signal amplification strategy based on target amplification and detection signal amplification is expected to achieve highly sensitive detection of microRNAs.

Here, we combined a dual signal amplification strategy of HCR and EIM from the perspectives of target amplification and detection signal amplification with ASV to construct an ultrasensitive electrochemical sensor for detection of microRNA-21 (Scheme 1). The sensor exhibited a good linear relationship between the current signal and logarithmic concentration of microRNA-21 in the range of 2.5 fM to 25 nM with a detection limit as low as 0.12 fM. The main reasons that the sensor showed an excellent performance were as follows: (1) HCR could expand microRNA-21 into longer nucleic acids polymers and provide more binding sites of enzymes, which effectively achieved the amplification of target; (2) Much Ag^0 was deposited on the electrode due to the EIM, which effectively achieved the amplification of detection signal; (3) Sensitive ASV was performed to detect microRNA-21 by keeping a record of stripping signals of silver. In addition, the uniform AuNPs modified ITO microelectrode array (MA) was constructed to put multiple samples.

2. Experimental section

2.1. Chemicals and apparatus

Alkaline-phosphatase-labeled streptavidin (SA-ALP) was purchased from Vector (Burlingame, CA). Poly (dimethylsiloxane) (PDMS, RTV615A and RTV615B) was purchased from GE (GE Toshiba Silicones. Co., Ltd., Japan). *N*-(3-dimethylaminopropyl)-*N′*-ethylcarbodiimide hydrochloride (EDC), 2-(N-Morpholino) ethanesulfonic acid (MES), 3-aminopropyltriethoxysilane (APTES), $HAuCl_4$ and bovine serum albumin (BSA) were purchased from Sigma-Aldrich. The p-nitrophenol sodium phosphate hexahydrate (p-NPP) and p-aminophenyl phosphate monohydrate (p-APP) were purchased from Santa Cruz Biotechnology, Inc. Diethyl dicarbonate (DEPC) treated water was purchased from Shanghai Sangon Biotech (China). All other chemical reagents were purchased from Sinopharm Chemical Reagent Co., Ltd. (Shanghai, China). All the nucleic acids sequences purified with HPLC were received from Shanghai Sangon Biotech (China), which were shown in Table S1.

UV-2550 (Shimadzu, Japan) spectrophotometer was used to acquire UV–vis absorption spectra. Dynamic light scattering (DLS) measurements were performed on a Zetasizer Nano ZS instrument (Malvern).

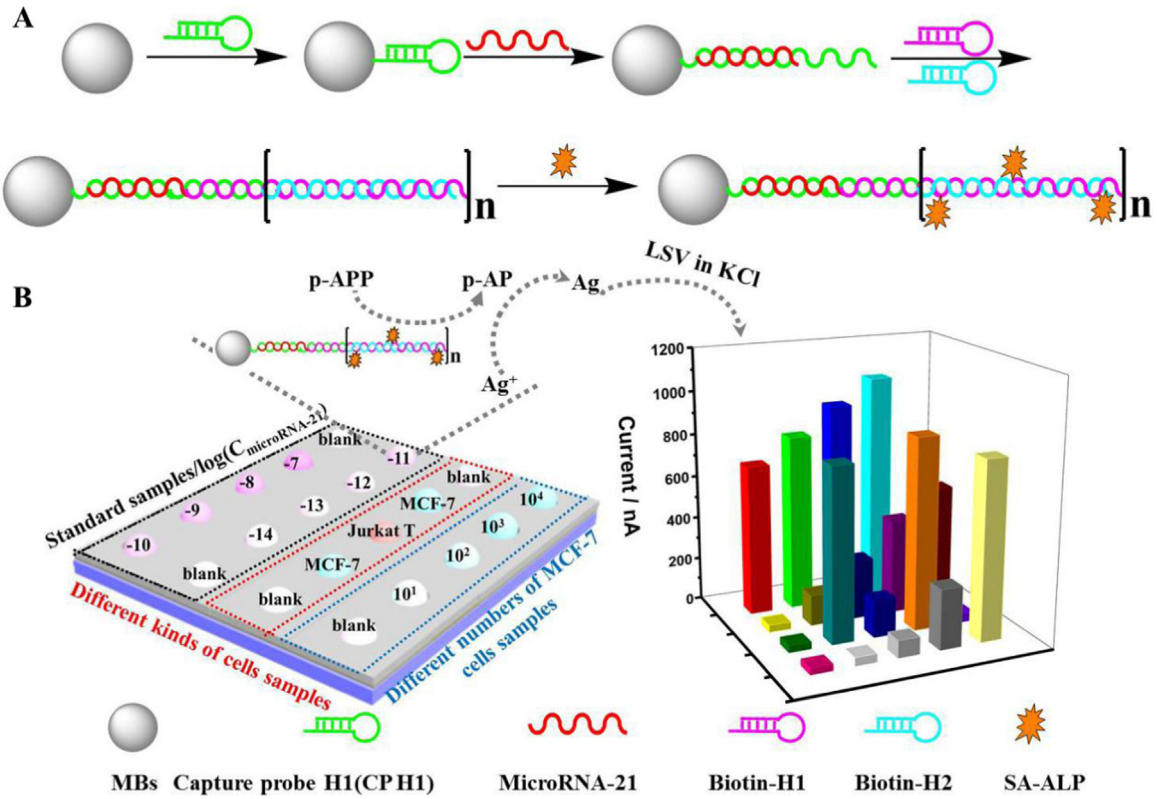

Scheme 1. Illustration of the protocol for electrochemical detection of microRNA-21: (A) Capture of microRNA-21 and HCR. (B) EIM and electrochemical detection of multiple samples on the same MA.

All electrochemical assays were performed on a CHI660a electrochemical workstation (CH Instruments, Inc. Shanghai, China), which used Ag/AgCl as reference electrode and platinum wire as counter electrode. TEM (FEI Tecnai G2 20 TWIN) was performed to obtain the morphology of magnetic nanobeads (MBs) and AuNPs. SEM images were acquired on a ZEISS SIGMA FESEM.

2.2. Preparation of AuNPs modified ITO microelectrode array (MA)

MA was fabricated according to the literatures (Young et al., 2016; Wu et al., 2018). AuNPs were prepared by sodium citrate reduction method and concentrated by ultrafiltration. The fabrication process of MA was shown in Fig. S1. First of all, the ITO glasses were cut into $2 \times 2\,cm^2$ square pieces. After washing with ultrapure water, the glasses were dried with N_2 and then soaked in piranha (7:3, (v/v) concentrated H_2SO_4/30% H_2O_2) solution for about 5 min to achieve further cleaning [Caution! The piranha solution should be handled with extreme care]. Next, the ITO glasses were put into the mixed solution of 10 mL water, 4 mL methanol, 20 μL acetic acid and 300 μL APTES under the condition of 37 °C for 2 h with gentle shaking. Subsequently, the AuNPs modified ITO glasses were obtained by placing ITO glasses in the mixed solution of 800 μL 0.01 M PBS (PH = 7.2), 4 μL 10 mM EDC and 40 μL AuNPs with gentle shaking for 15 min.

At the same time, 5 g PDMS (10:1, w/w, RTV615A/RTV615B) was mixed evenly and spin-coated on the silicon wafer by spin coater. After that, the silicon wafer was baked at 75 °C for 2 h to form PDMS membrane. Next, the PDMS membrane was cut into a rectangular section of $2 \times 1.5\,cm^2$. The MA were obtained by covering the PDMS membrane with an array of 1 mm diameter holes onto the surface of AuNPs modified ITO glasses.

2.3. Extraction of total RNA in cells

The total RNA were extracted from MCF-7 cells and Jurkat T cells according to the instruction of Eastep® Super Total RNA Extraction Kit. The cells were placed in a non-enzymatic centrifuge tube and were lysed by pyrolysis liquid. The supernatant were collected by centrifugal. After that, the supernatant was washed by ethanol and RNA lotion. Subsequently, DNA enzymes were added to remove excess DNA. At last, total RNA could be obtained by washing with RNA lotion and then stored at −70 °C for further use.

2.4. Preparation of magnetic nanobeads (MBs)-capture probe H1 (MBs-CP H1)

The MBs with good dispersion and excellent magnetic response were synthesized by using the assembly method previously reported by our group (Wen et al., 2014). The MBs-CP H1 were prepared based on the amidation reaction between the carboxyl group on the surface of the MBs and the amino group of the capture probe H1 (CP H1). After washing with MES, 40 μL MBs (11.0 mg/mL) were mixed with 50 μL 12 μM CP H1 and 0.2 mg EDC at 25 °C with gentle shaking (150 rpm) for 1 h. Then, 4 μL 100 mg/mL EDC was added to the mixed solution, which was kept at 25 °C with gentle shaking (150 rpm) overnight. Magnetic scaffold was used to adsorb MBs and remove the redundant CP H1. After washing with PBS for three times, the MBs-CP H1 were blocked with 1% BSA and stored at 4 °C for further use.

2.5. Ultrasensitive electrochemical detection of microRNA-21

Different concentrations of microRNA-21 standard samples or complex samples were reacted with 20 μL MBs-CP H1 at 25 °C for 1 h with gentle shaking (150 rpm), After washing three times, the MBs-CP H1/microRNA-21 complexes were redispersed into 80 μL PBS. Subsequently, 10 μL 1.2 μM biotin-H1 and 10 μL 1.2 μM biotin-H2 were added to the solution, continuing reaction at 25 °C for 2 h with gentle shaking (150 rpm). After repeat washing to remove excess biotin-H1 and biotin-H2, the MBs-CP H1/microRNA-21/biotin-H1/biotin-H2 complexes were reacted with 100 μL 1 μg/mL SA-ALP at 25 °C for 30 min. Removing the redundant SA-ALP, and washing for three times, the MBs-CP H1/microRNA-21/biotin-H1/biotin-H2/SA-ALP were mixed with p-APP and $AgNO_3$, and then added rapidly into MA for reaction for 30 min. Then, MA was gently flushed with water. At last, 1 μL 0.1 M KCl were added in each microelectrode, respectively. The electrochemical tests were based on a three-electrode system, in which MA was used as the working electrode, the Ag/AgCl and the platinum wire were used as the reference electrode and the counter electrode, respectively. The dissolved voltammetric currents of silver were collected based on linear sweep voltammetry (LSV) performed within −0.1 V~0.3 V, with a sweep rate of 0.1 V/S.

3. Results and discussion

3.1. Characterization of MA

MA was prepared based on the covalent coupling reaction between carboxyl groups on the surface of AuNPs and amino groups on the surface of ITO glasses. AuNPs with uniform particle size of 15.8 nm and rich carboxyl groups were coupled with ITO glasses (Fig. S2). The surface morphology of microelectrodes was characterized by SEM. AuNPs presented the characteristics of submonolayer and uniform arrangement on the ITO slides (Fig. 1A). The cyclic voltammograms (CV) curve of the microelectrode in H_2SO_4 indicated that AuNPs were successfully modified on ITO glasses (Fig. 1B). The electroactive area of the microelectrode was calculated to be $0.186\,mm^2$. Fig. 1C showed the CV curves of an AuNPs modified ITO microelectrode and an unmodified ITO microelectrode in $[Fe(CN)_6]^{3-/4-}$. It was observed that the peak current was significantly enhanced by AuNPs. And the CV curves of the five randomly selected microelectrodes in $[Fe(CN)_6]^{3-/4-}$ (Fig. 1D) were basically coincident (peak current, relative standard deviation (RSD) = 0.82%), which proved that the MA had uniform electrochemical response and good repeatability.

3.2. Fabrication and characterization of MBs-CP H1

MBs are easier to operate and separate due to rapid magnetic response. The uniform and dispersive MBs were synthesized by layer-by-layer assembly method, with an average particle size of 281 nm (Fig. 2A, B). The magnetic response of MBs was tested according to the capture efficiency of MBs in different time with a magnetic scaffold (Fig. 2C). The results showed that almost all the MBs could be captured in 90 s, which had a rapid magnetic response and could achieve rapid separation. The coupling of CP H1 and MBs based on amidation reaction resulted in a negative shift of the surface potential from −11.5 mV to −46.4 mV (Fig. 2D). In addition, the absorption of CP H1 in the supernatant at 260 nm decreased significantly compared to the added CP H1 after the reaction (Fig. S3), which further proved the successful coupling of CP H1 with MBs. The numbers of CP H1 per MB were calculated to be 102 according to the standard curve of MBs and CP H1 (Fig. S4A, B), which could achieve efficient capture of microRNA-21.

3.3. Signal amplification of hybridization chain reaction (HCR)

The feasibility of HCR was verified by agarose gel electrophoresis. As shown in Fig. S5, microRNA-21 could react with CP H1 and then long dsDNA were formed (Lane 3). With the addition of biotin-H1 and biotin-H2, the generation of longer dsDNA proved the occurrence of HCR (Lane 4). However, in the absence of microRNA-21, no long nucleic acids were observed (Lane 5). In addition, the amplification effect of HCR was further investigated based on the characteristic absorption at 405 nm generated by the catalysis of ALP (Fig. 3A). After the target was captured by MBs-CP H1, biotin-H1 and biotin-H2 were added

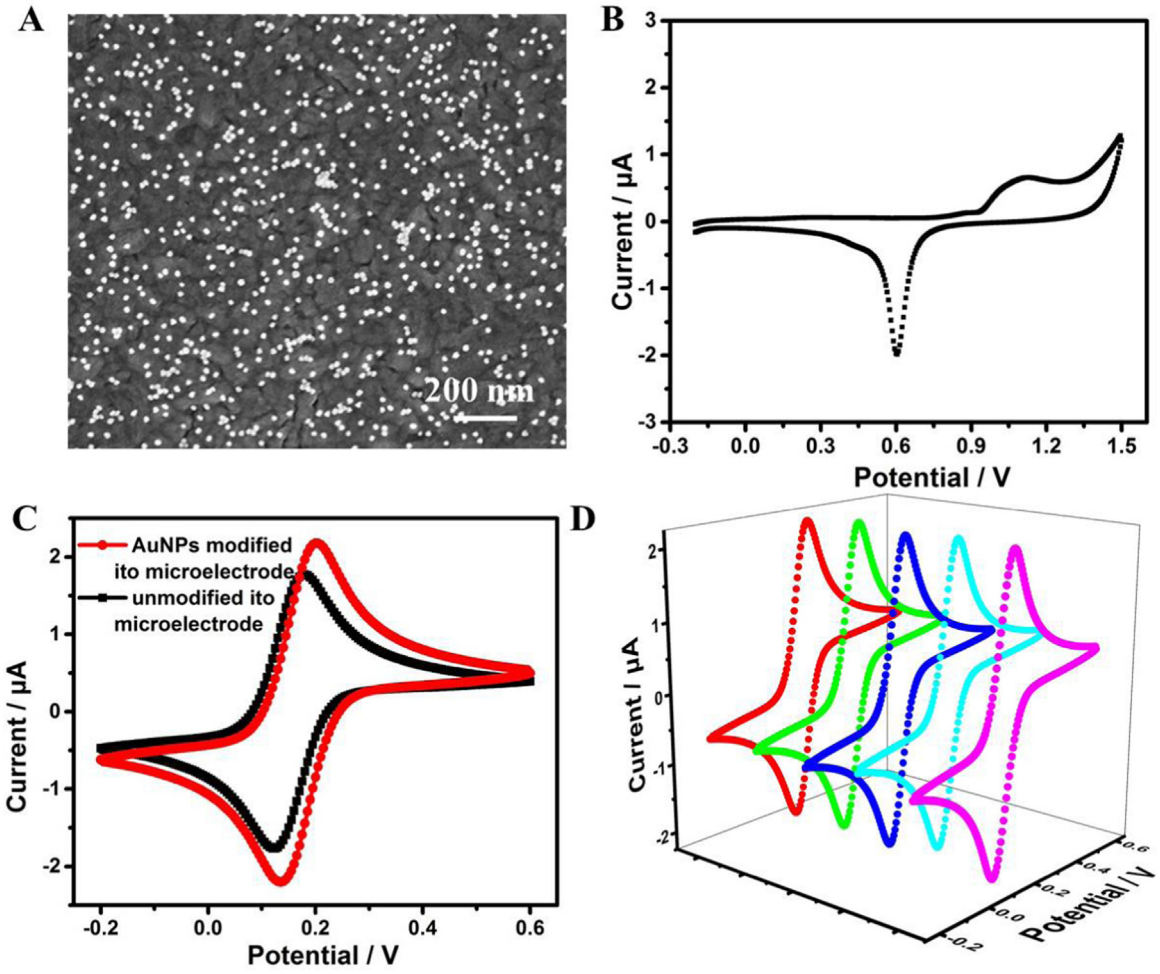

Fig. 1. Characterization of MA. (A) SEM image of MA. (B) CV curve of a microelectrode in 0.5 M H_2SO_4. (C) CV curves of an AuNPs modified ITO microelectrode and an unmodified ITO microelectrode in $[Fe(CN)_6]^{3-/4-}$. (D) CV curves of five parallel microelectrodes in $[Fe(CN)_6]^{3-/4-}$.

together indicating the presence of HCR, whereas only biotin-H2 was added indicating the absence of HCR. Then, ALP were coupled based the specific reaction between biotin and streptavidin. The occurrence of HCR greatly increased the number of coupled ALP. Then stronger absorption at 405 nm was observed. At the same time, more significant color change was observed with the naked eye (Fig. S6). Moreover, when microRNA-21 existed in the solution, the ultraviolet absorption was stronger than the solution without microRNA-21 (Fig. 3A). UV spectra and photographs from Fig. 3A and S6 showed that microRNA-21 was successfully amplified by HCR.

3.4. Electrochemical signal amplification of enzyme-induced metallization (EIM)

EIM was incorporated into HCR to achieve further signal amplification. Based on the specific effect between biotin and streptavidin, multiple ALP molecules were conjugated to the nucleic acids polymers produced by HCR. ALP catalyzed substrate p-APP to produce p-aminophenol (p-AP), which could react with Ag^+ as a reductant to produce Ag^0 depositing on the electrode surface. At last, microRNA-21 could be detected by the dissolving signal of Ag^0. Significant current was observed when microRNA-21 was present (Fig. S7A), indicating a high signal-to-background ratio of the method. In order to confirm the amplification effects of EIM and HCR, respectively, we detect microRNA-21 under different reaction conditions. The current was negligible, which indicated Ag^0 could not be deposited by p-APP only (Fig. 3B, curve black). However, with the introduction of ALP, a nearly 40-fold increase of current could be observed (Fig. 3B, curve red), indicating an efficient amplification of detection signal by EIM. Then, the combination of HCR could amplify the current by about 3-fold under the same concentration of microRNA-21 (Fig. 3B, curve blue), which achieved amplification of microRNA-21. As shown in Fig. S7B, the currents obtained by three parallel tests were recorded. Overall, a dual signal amplification strategy of HCR and EIM effectively enhanced electrochemical signal by nearly 120-fold. The main reasons were as follows: (1) The HCR rapidly expanded the target into a long nucleic acids polymers and provided a large number of enzyme binding sites; (2) The EIM combined the high specificity of the enzyme with the high sensitivity of nanoparticle labels in combination with metal enhancement, which realized the direct amplification of signal; (3) Anodic stripping voltammetry (ASV) was combined with EIM to achieve a more sensitive detection signal. In summary, the integration of dual signal amplification of EIM and HCR with ASV could effectively realize signal amplification and achieve sensitive detection of microRNA-21. The best signal-to-background ratio could be obtained as the concentrations of SA-ALP, p-APP and Ag^+ were 1 μg/mL, 3 mM and 12.5 μM, respectively (Fig. S8A, B and C). In addition, the optimal enzymatic reaction time was 30 min (Fig. S8D).

3.5. Ultrasensitive detection of microRNA-21 with a wide linear dynamic range

Based on the combination of a dual signal amplification of HCR and EIM with ASV, an electrochemical sensor for microRNA-21 was

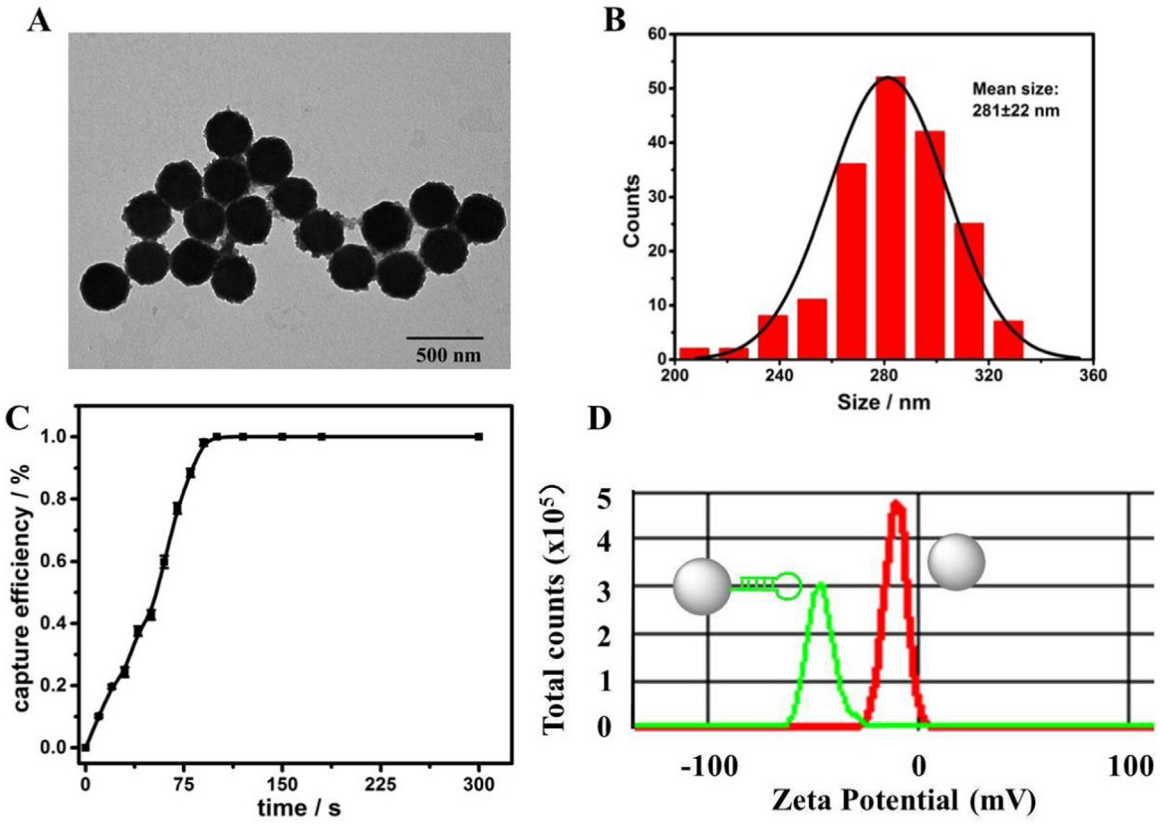

Fig. 2. (A) TEM image of MBs. (B) Size distribution of MBs. (C) Magnetic response test of MBs. (D) Zeta potential of MBs and MBs-CP H1.

constructed. Multiple groups of standard samples and cell samples could all be put on the same MA, which realized the detection of standard and cells samples synchronously (Fig. 4A). As shown in Fig. 1D and Fig. S9A, the MA with good repeatability and uniform performance was fabricated for the detection of multiple samples. Subsequently, the currents at different concentrations of microRNA-21 were recorded (Fig. 4B, C). As shown in Fig. 4D, there was a good linear relationship between the current and logarithmic concentration of microRNA-21 in the range of 2.5 fM to 25 nM with a detection limit of 0.12 fM ($S/N = 3$). The combination of a dual signal amplification strategy of HCR and EIM with ASV made the method highly sensitive. Compared with the previous reports (Table S2), this method was not only highly sensitive, but also had a wider detection range spanning 7 orders of magnitude, which could meet the requirement of wide range detection of microRNAs. At the same time, the MA had successfully been used for the detection of multiple samples, which had a good repeatability.

It is worth noting that microRNAs are highly homologous, which requires the detection methods to be highly specific. To evaluate the specificity of the present sensor, the same concentration of microRNA-21 (T) and single-base mismatched sequence (MT1) and double-base mismatched sequence (MT2) were detected by this method. The electrochemical signal of microRNA-21 was almost twice that of MT1, and three times that of MT2 (Fig. S9B), which proved that this method had a good specificity to distinguish the mismatched sequences.

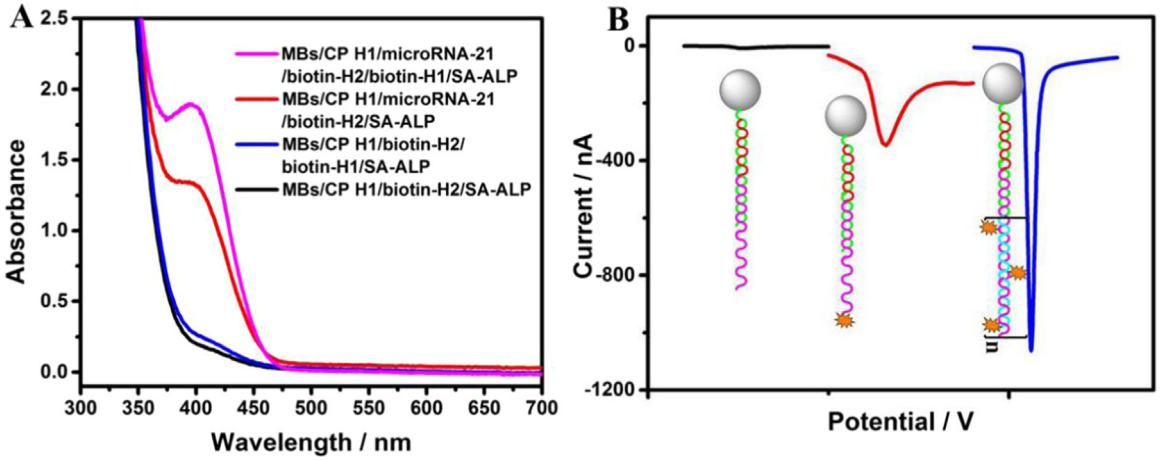

Fig. 3. (A) UV–vis absorption spectra of the supernatant under different conditions. (B) LSVs under different conditions in 0.1 M KCl: MBs/CP H1/microRNA-21/biotin-H2 (curve black); MBs/CP H1/microRNA-21/biotin-H2/SA-ALP (curve red); MBs/CP H1/microRNA-21/biotin-H2/biotin-H1/SA-ALP (curve blue).

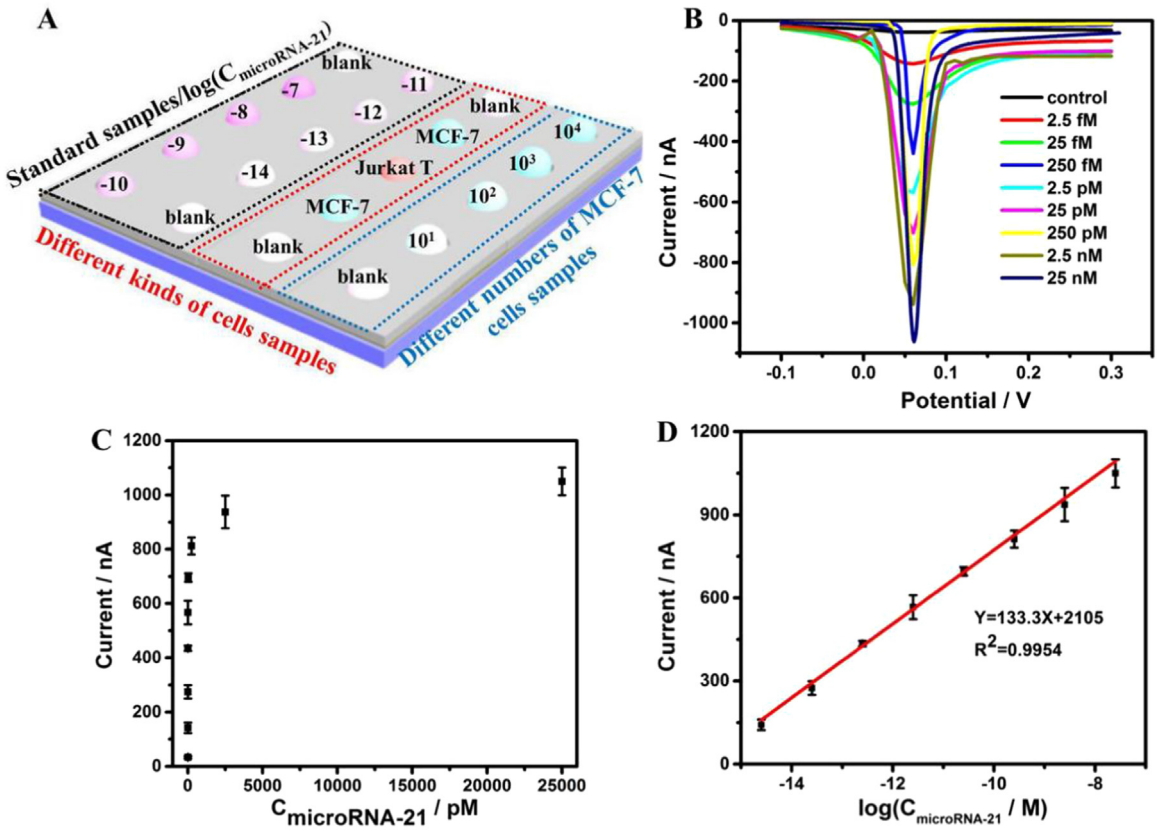

Fig. 4. (A) Scheme of detection of multiple samples on the same MA. (B) Typical LSV signals in the presence of different microRNA-21 concentrations. (C) The plot of current intensity vs. the concentration of microRNA-21. (D) The linear relationship between the current intensity and the logarithm of microRNA-21 concentration.

3.6. Detection of microRNA-21 in complex samples

The detection of real samples was an important factor to evaluate the analytical performance of the method. Firstly, the developed biosensor was used to detect microRNA-21 in human serum samples from the Zhongnan Hospital of Wuhan University by the method of standard addition. As shown in Table S3, the recoveries from 96% to 104.8% were obtained, indicating a good performance of the biosensor in human serum. We further applied the electrochemical sensor to detect the content of microRNA-21 in various amounts of MCF-7 cells associated with human breast cancer. As shown in Fig. 5A, the current obtained from 10 MCF-7 cells was indistinguishable from the blank one. But the current intensity was stronger when the amounts of MCF-7 cells increased to 100, indicating that the method also had excellent sensitivity to cells. Furthermore, the electrochemical sensor was used to detect the content of microRNA-21 in MCF-7 cells and Jurkat T cells. Compared with current obtained from Jurkat T cells, more significant current obtained from MCF-7 cells was observed, proving the over expression of microRNA-21 in MCF-7 cells (Fig. 5B). In a word, the electrochemical sensor had excellent performance in the detection of microRNA-21 in complex samples.

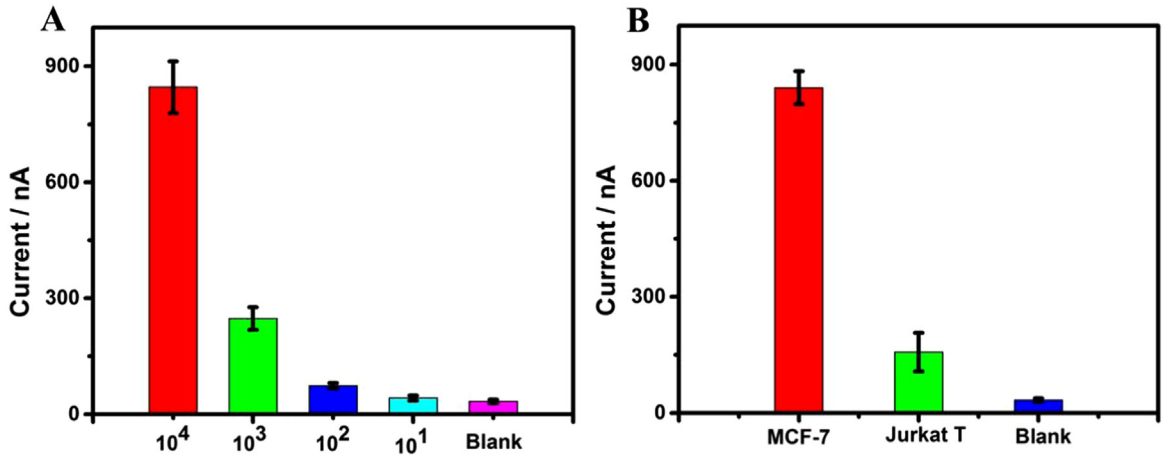

Fig. 5. (A) Histogram for microRNA-21 expression level in various amounts of MCF-7 cells. (B) Histogram for microRNA-21 expression level in MCF-7 cells and Jurkat T cells.

4. Conclusions

In summary, an ultrasensitive electrochemical biosensor for microRNA-21 based on the combination of a dual signal amplification strategy with ASV has been demonstrated. A dual signal amplification strategy was realized by using HCR for target amplification and EIM for detection signal amplification, which could amplify current by 120-fold. As low as 0.12 fM microRNA-21 could be detected with high sensitivity and specificity and a wide linear range from 2.5 fM to 25 nM was obtained spanning 7 orders of magnitude. The developed biosensor was also used to the detection of microRNA-21 in cells, showing a great potential for microRNAs detection in complex samples and providing a possibility for early diagnosis of the diseases.

CRediT authorship contribution statement

Wen-Jing Guo: Investigation, Methodology, Writing - original draft, Writing - review & editing. **Zhen Wu:** Investigation, Writing - original draft. **Xiao-Yan Yang:** Investigation. **Dai-Wen Pang:** Methodology, Resources. **Zhi-Ling Zhang:** Methodology, Resources, Supervision, Writing - original draft, Writing - review & editing, Funding acquisition.

Acknowledgments

This work was supported by the National Natural Science Foundation of China (21775111, 21475099) and the National Science and Technology Major Project of China (2018ZX10301405).

Declaration of interests

The authors declare that they have no known competing financial interests or personal relationships that could have appeared to influence the work reported in this paper.

Appendix A. Supporting information

Supplementary data associated with this article can be found in the online version at doi:10.1016/j.bios.2019.02.026.

References

Alfonta, L., Singh, A.K., Willner, I., 2001. Anal. Chem. 73, 91–102.
Brennecke, J., Hipfner, D.R., Stark, A., Russell, R.B., Cohen, S.M., 2003. Cell 113, 25–36.
Dirks, R.M., Pierce, N.A., 2004. PNAS 101, 15275–15278.
Folini, M., Gandellini, P., Longoni, N., Profumo, V., Callari, M., Pennati, M., Colecchia, M., Supino, R., Veneroni, S., Salvioni, R., 2010. Mol. Cancer 9, 1–12.
Frankel, L.B., Christoffersen, N.R., Jacobsen, A., Lindow, M., Krogh, A., Lund, A.H., 2008. J. Biol. Chem. 283, 1026–1033.
Galina, G., Thomas, W., Santosh, K., Esau, C.C., Julja, B., Linsley, P.S., Krichevsky, A.M., 2008. Mol. Cell. Biol. 28, 5369–5380.
Gao, L.Z., Zhuang, J., Nie, L., Zhang, J.B., Zhang, Y., Gu, N., Wang, T.H., Feng, J., Yang, D.L., Perrett, S., Yan, X., 2007. Nat. Nanotechnol. 2, 577–583.
Ge, Z., Lin, M., Wang, P., Pei, H., Yan, J., Shi, J., Huang, Q., He, D., Fan, C., Zuo, X., 2014. Anal. Chem. 86, 2124–2130.
Hou, T., Li, W., Liu, X., Li, F., 2015. Anal. Chem. 87, 11368–11374.
Hwang, S., Kim, E., Kwak, J., 2005. Anal. Chem. 77, 579–584.
Johnston, R.J., Hobert, O., 2003. Nature 426, 845–849.
Jung, S., Kim, B.K., Lee, S., Yoon, S., Im, H.-I., Kim, S.K., 2018. Sens. Actuators B. 262, 118–124.
Lu, J., Getz, G., Miska, E.A., Alvarez-Saavedra, E., Lamb, J., Peck, D., Sweet-Cordero, A., Ebert, B.L., Mak, R.H., Ferrando, A.A., Downing, J.R., Jacks, T., Horvitz, H.R., Golub, T.R., 2005. Nature 435, 834–838.
Mansourian, N., Rahaie, M., Hosseini, M., 2017. J. Fluoresc. 27, 1679–1685.
Park, S.J., Taton, T.A., Mirkin, C.A., 2002. Science 295, 1503–1506.
Robert, M., Richard, D.P., James, F.H., Wolfgang, F., 2005. Nano Lett. 5, 1475–1482.
Rochelet-Dequaire, M., Djellouli, N., Limoges, B., Brossier, P., 2009. Analyst 134, 349–353.
Rui, S., Chiang, V.L., 2005. BioTechniques 39, 519–525.
Salamin, O., Kuuranne, T., Saugy, M., Leuenberger, N., 2017. Drug Test. Anal. 9, 1731–1737.
Shirley, T., Richard, D.B., Ming-Sound, T., Mcpherson, J.D., 2014. Lab. Invest. 94, 350–358.
Tang, S., Gu, Y., Lu, H., Dong, H., Zhang, K., Dai, W., Meng, X., Yang, F., Zhang, X., 2018. Anal. Chim. Acta 1004, 1–9.
Thomson, J.M., Parker, J., Perou, C.M., Hammond, S.M., 2004. Nat. Methods 1, 47–53.
Torrente-Rodríguez, R.M., Campuzano, S., Montiel, V.R.-V., Montoya, J.J., Pingarrón, J.M., 2016. Biosens. Bioelectron. 86, 516–521.
Varallyay, E., Burgyan, J., Havelda, Z., 2008. Nat. Protoc. 3, 190–196.
Wen, C.Y., Wu, L.L., Zhang, Z.L., Liu, Y.L., Wei, S.Z., Hu, J., Tang, M., Sun, E.Z., Gong, Y.P., Yu, J., 2014. ACS Nano 8, 941–949.
Wienholds, E., Kloosterman, W.P., Miska, E., Alvarez-Saavedra, E., Berezikov, E., de Bruijn, E., Horvitz, H.R., Kauppinen, S., Plasterk, R.H.A., 2005. Science 309, 310–311.
Wightman, B., Ha, I., Ruvkun, G., 1993. Cell 75, 855–862.
Wu, Z., Guo, W.J., Bai, Y.Y., Zhang, L., Hu, J., Pang, D.W., Zhang, Z.L., 2018. Anal. Chem. 90, 1683–1690.
Wu, Z., Zhou, C.H., Pan, L.J., Zeng, T., Zhu, L., Pang, D.W., Zhang, Z.L., 2016. Anal. Chem. 88, 9166–9172.
Xu, H., Wu, D., Zhang, Y., Shi, H., Ouyang, C., Li, F., Jia, L., Yu, S., Wu, Z.-S., 2018. Sens. Actuators B 258, 470–477.
Yang, L., Liu, C.H., Ren, W., Li, Z.P., 2012. ACS Appl. Mater. Interfaces 4, 6450–6453.
Yang, Q., Gu, W.W., Gu, Y., Yan, N.N., Mao, Y.Y., Zhen, X.X., Wang, J.M., Yang, J., Shi, H.J., Zhang, X., 2018. J. Transl. Med. 16, 186.
Yao, Q., Xu, H., Zhang, Q.Q., Zhou, H., Qu, L.H., 2009. Biochem. Biophys. Res. Commun. 388, 539–542.
Young, S.L., Kellon, J.E., Hutchison, J.E., 2016. J. Am. Chem. Soc. 138, 13975–13984.
Yu, X., Zhang, Z.L., Zheng, S.Y., 2015. Biosens. Bioelectron. 66, 520–526.
Yuan, Y.H., Wu, Y.D., Chi, B.Z., Wen, S.H., Liang, R.P., Qiu, J.D., 2017. Biosens. Bioelectron. 97, 325–331.
Zhang, J.G., Wang, J.J., Zhao, F., Liu, Q., Jiang, K., Yang, G.H., 2010. Clin. Chim. Acta 411, 846–852.
Zhang, Z., Li, Z., Gao, C., Chen, P., Chen, J., Liu, W., Xiao, S., Lu, H., 2008. Lab. Investig. 88, 1358–1366.
Zhou, C.H., Wu, Z., Chen, J.J., Xiong, C., Chen, Z., Pang, D.W., Zhang, Z.L., 2015. Chem. - Asian J. 10, 1387–1393.
Zhou, C.H., Zhao, J.Y., Pang, D.W., Zhang, Z.L., 2014. Anal. Chem. 86, 2752–2759.